

REPORT DOCUMENTATION PAGE

Form Approved OMB NO. 0704-0188

The public reporting burden for this collection of information is estimated to average 1 hour per response, including the time for reviewing instructions, searching existing data sources, gathering and maintaining the data needed, and completing and reviewing the collection of information. Send comments regarding this burden estimate or any other aspect of this collection of information, including suggestions for reducing this burden, to Washington Headquarters Services, Directorate for Information Operations and Reports, 1215 Jefferson Davis Highway, Suite 1204, Arlington VA, 22202-4302. Respondents should be aware that notwithstanding any other provision of law, no person shall be subject to any penalty for failing to comply with a collection of information if it does not display a currently valid OMB control number.
PLEASE DO NOT RETURN YOUR FORM TO THE ABOVE ADDRESS.

1. REPORT DATE (DD-MM-YYYY) 27-04-2012	2. REPORT TYPE Final Report	3. DATES COVERED (From - To) 1-Oct-2007 - 31-Jan-2012
-------------------------------------------	--------------------------------	----------------------------------------------------------

4. TITLE AND SUBTITLE Chemical Communications - Final Report	5a. CONTRACT NUMBER W911NF-07-1-0647
	5b. GRANT NUMBER
	5c. PROGRAM ELEMENT NUMBER 7620AK

6. AUTHORS L. Mahadevan, David Walt, George M. Whitesides	5d. PROJECT NUMBER
	5e. TASK NUMBER
	5f. WORK UNIT NUMBER

7. PERFORMING ORGANIZATION NAMES AND ADDRESSES Harvard University Office of Sponsored Research 1350 Massachusetts Ave. Holyoke 727 Cambridge, MA 02138 -	8. PERFORMING ORGANIZATION REPORT NUMBER
----------------------------------------------------------------------------------------------------------------------------------------------------------------------	------------------------------------------

9. SPONSORING/MONITORING AGENCY NAME(S) AND ADDRESS(ES) U.S. Army Research Office P.O. Box 12211 Research Triangle Park, NC 27709-2211	10. SPONSOR/MONITOR'S ACRONYM(S) ARO
	11. SPONSOR/MONITOR'S REPORT NUMBER(S) 53391-MS-DRP.11

12. DISTRIBUTION AVAILABILITY STATEMENT
Approved for Public Release; Distribution Unlimited

13. SUPPLEMENTARY NOTES
The views, opinions and/or findings contained in this report are those of the author(s) and should not be construed as an official Department of the Army position, policy or decision, unless so designated by other documentation.

14. ABSTRACT
Systems based on infochemistry combine the storage and transmission of encoded information with four attractive features of chemistry: i) high energy density; ii) autonomous generation of power that can be used for both sensing and for transmission; iii) no requirement for batteries; iv) facile coupling with certain kinds of chemical sensing.

Throughout the infochemistry project, the Walt laboratory, at Tufts University, was responsible for developing an

15. SUBJECT TERMS
alphanumeric characters; bubble shutter; infofuse; IR detection; IR emission; optical transmission; atomic emission beacon; info biology

16. SECURITY CLASSIFICATION OF:			17. LIMITATION OF ABSTRACT UU	15. NUMBER OF PAGES	19a. NAME OF RESPONSIBLE PERSON George Whitesides
a. REPORT UU	b. ABSTRACT UU	c. THIS PAGE UU			19b. TELEPHONE NUMBER 617-495-9430

Report Title

Chemical Communications - Final Report

ABSTRACT

Systems based on infochemistry combine the storage and transmission of encoded information with four attractive features of chemistry: i) high energy density; ii) autonomous generation of power that can be used for both sensing and for transmission; iii) no requirement for batteries; iv) facile coupling with certain kinds of chemical sensing.

Throughout the infochemistry project, the Walt laboratory, at Tufts University, was responsible for developing an instrument/detector to observe the emission signals from the burning fuse developed in the Whitesides laboratory, at Harvard. We developed multiple systems for the project.

In this final report, we summarize and outline the accomplishments of the project.

Enter List of papers submitted or published that acknowledge ARO support from the start of the project to the date of this printing. List the papers, including journal references, in the following categories:

(a) Papers published in peer-reviewed journals (N/A for none)

<u>Received</u>	<u>Paper</u>
-----------------	--------------

TOTAL:

Number of Papers published in peer-reviewed journals:

(b) Papers published in non-peer-reviewed journals (N/A for none)

<u>Received</u>	<u>Paper</u>
-----------------	--------------

TOTAL:

Number of Papers published in non peer-reviewed journals:

(c) Presentations

Palacios, M. A.; Walt, D R.: InfoBiochemistry: Arrays of microorganisms' colonies for timed release of encrypted messages. Bioanalytical Sensors, Gordon Research Conference, 2010.

Palacios, M. A.; Benito-Peña, E.; Manesse, M. A.; LaFratta, C. N.; Mazzeo, A.; Whitesides, G. M.; Walt, D. InfoChemistry: Bioencrypted messages in arrays of E.coli by cytosolic expression of fluorescent proteins. American Chemical Society Meeting: Boston MA, 2010.

Lafratta, C. "Infochemistry: Sending encoded messages using combustion from atomic beacons" 12th Annual Mid-Hudson American Chemical Society Undergraduate Research Symposium, Bard College, Annandale-on-Hudson, NY 12504, April 13th, 2011

Number of Presentations: 3.00

Non Peer-Reviewed Conference Proceeding publications (other than abstracts):

Received Paper

TOTAL:

Number of Non Peer-Reviewed Conference Proceeding publications (other than abstracts):

Peer-Reviewed Conference Proceeding publications (other than abstracts):

Received Paper

TOTAL:

Number of Peer-Reviewed Conference Proceeding publications (other than abstracts):

(d) Manuscripts

Received Paper

02/03/2009 1.00 S.W. Thomas III, R.C. Chiechi, C.N. LaFratta, M.R. Webb, others, see report, George M. Whitesides.
Infochemistry and Infofuses: Chemical Storage and Transfer of Coded Information,
()

TOTAL: **1**

Number of Manuscripts:

Books

Received

Paper

TOTAL:

Patents Submitted

Submitted:

~~"Systems and Methods for Amplification and Phage Display", Derda, R., Tang, S.K.Y., Whitesides, G.M. PCT/US11/39932~~

"Method for Measuring "closeness" in a Network", Mahadevan, L., Morrison, G.C. 13/230,496

Patents Awarded

Awards

Whitesides:

King Feisal Prize in Science (Saudi Arabia) (2011)

F. A. Cotton Award (Texas ACS Section) (2011)

Priestley Award (Dickenson College) (2011)

Mahadevan:

Singleton Lecturer, MIT (2010)

Amick Lecturer, U Chicago (2011)

Walt:

University of Michigan Distinguished Innovator Lecture (2010)

Stony Brook University Distinguished Alumni Award (2010)

American Chemical Society National Award for Creative Invention (2010)

Graduate Students

<u>NAME</u>	<u>PERCENT SUPPORTED</u>	Discipline
Jian (Jerry) Guo	0.67	
Sindy Kam Yan Tang	1.00	
FTE Equivalent:	1.67	
Total Number:	2	

Names of Post Doctorates

<u>NAME</u>	<u>PERCENT SUPPORTED</u>
Chris LaFratta	0.25
Mael Manesse	0.20
Manuel Palacios	0.33
Michael Webb	0.20
Huaibin (Eli) Zhang	0.15
Sarah Bruner	0.20
Kyeng Min Park	1.00
Alex Nemiroski	1.00
Hyo Jae Yoon	1.00
Aaron Mazzeo	0.25
Claudiu Stan	0.10
Rui Nunes	1.00
Siowling Soh	0.50
Stephen Morin	0.25
FTE Equivalent:	6.43
Total Number:	14

Names of Faculty Supported

<u>NAME</u>	<u>PERCENT SUPPORTED</u>	National Academy Member
George M. Whitesides	0.10	Yes
L. Mahadevan	0.08	
David Walt	0.10	
FTE Equivalent:	0.28	
Total Number:	3	

Names of Under Graduate students supported

<u>NAME</u>	<u>PERCENT SUPPORTED</u>
FTE Equivalent:	
Total Number:	

Student Metrics

This section only applies to graduating undergraduates supported by this agreement in this reporting period

- The number of undergraduates funded by this agreement who graduated during this period: 0.00
- The number of undergraduates funded by this agreement who graduated during this period with a degree in science, mathematics, engineering, or technology fields:..... 0.00
- The number of undergraduates funded by your agreement who graduated during this period and will continue to pursue a graduate or Ph.D. degree in science, mathematics, engineering, or technology fields:..... 0.00
- Number of graduating undergraduates who achieved a 3.5 GPA to 4.0 (4.0 max scale):..... 0.00
- Number of graduating undergraduates funded by a DoD funded Center of Excellence grant for Education, Research and Engineering:..... 0.00
- The number of undergraduates funded by your agreement who graduated during this period and intend to work for the Department of Defense 0.00
- The number of undergraduates funded by your agreement who graduated during this period and will receive scholarships or fellowships for further studies in science, mathematics, engineering or technology fields: 0.00

Names of Personnel receiving masters degrees

NAME

Total Number:

Names of personnel receiving PHDs

NAME

Jian (Jerry) Guo
Sindy Kam Yan Tang
Michinao Hashimoto

Total Number: 3

Names of other research staff

NAME

PERCENT SUPPORTED

T.J. Martin 0.25

Melissa LeGrand 0.25

FTE Equivalent: 0.50

Total Number: 2

Sub Contractors (DD882)

1 a. Tufts University

1 b. Office of the Vice Provost

Tufts University

Medford MA 021555807

Sub Contractor Numbers (c):

Patent Clause Number (d-1):

Patent Date (d-2):

Work Description (e):

Sub Contract Award Date (f-1): 10/1/2007 12:00:00AM

Sub Contract Est Completion Date(f-2): 1/31/2012 12:00:00AM

1 a. Tufts University

1 b. Grants and Contracts Administration

20 Professors Row

Medford MA 02155

Sub Contractor Numbers (c):

Patent Clause Number (d-1):

Patent Date (d-2):

Work Description (e):

Sub Contract Award Date (f-1): 10/1/2007 12:00:00AM

Sub Contract Est Completion Date(f-2): 1/31/2012 12:00:00AM

Inventions (DD882)

5 Method for Measuring "closeness" in a Network

Patent Filed in US? (5d-1) Y
Patent Filed in Foreign Countries? (5d-2) N
Was the assignment forwarded to the contracting officer? (5e) Y
Foreign Countries of application (5g-2):

5a: Lakshminarayanan Mahadevan

5f-1a: President and Fellows of Harvard College

5f-c: 60 Oxford Street
Cambridge MA 02138

5a: Gregory C. Morrison

5f-1a: President and Fellows of Harvard College

5f-c: 60 Oxford Street
Cambridge MA 02138

5 Systems and Methods for Amplification and Phage Display

Patent Filed in US? (5d-1) Y
Patent Filed in Foreign Countries? (5d-2) N
Was the assignment forwarded to the contracting officer? (5e) Y
Foreign Countries of application (5g-2):

5a: Sindy K.Y. Tang

5f-1a: President and Fellows of Harvard College

5f-c: 12 Oxford Street
Cambridge MA 02138

5a: Ratmir Derda

5f-1a: President and Fellows of Harvard College

5f-c: 12 Oxford Street
Cambridge MA 02138

5a: George M. Whitesides

5f-1a: President and Fellows of Harvard College

5f-c: 12 Oxford Street
Cambridge MA 02138

Scientific Progress

Please see attachment -

Technology Transfer



CHEMICAL COMMUNICATIONS
W911NF-07-1-0647
FINAL REPORT
8/1/11 – 1/31/12

Dr. Gill Pratt
3701 North Fairfax Drive
Arlington VA 22203-1714

Technical POC: Dr. Gill Pratt, DARPA/DSO

Submission from:

George M. Whitesides
Department of Chemistry and Chemical Biology
Harvard University
Cambridge, MA 02138
gwhitesides@gmwgroup.harvard.edu
Tel: 617 495 9430
Fax: 617 495 9857

Laboratory Manager
TJ Martin
tjmartin@gmwgroup.harvard.edu
Tel: 617 495 9432
Fax: 617 495 9857

Contents

InfoFuse.....	2
Droplet Laser.....	4
Bubble Shutter	4
Summary of milestones for Phase I, II and no-cost extension.....	5
Tufts University	6
Infochemistry	6
Initial Detector System Screening.....	6
1 st Generation Filter-Based System.....	8
2 nd Generation Filter-Based System.....	8
1 st Generation Portable Message Decoding System.....	12
2 nd Generation Portable Message Decoding System.....	16
Conclusion.....	18
Atomic Emission Beacons	19
Infobiology (taken from PNAS 2011, 108(40), 16510-4.).....	21
References	29

InfoFuse

In our original design of infofuses from phase I, information was encoded as patterns of ions (Li⁺, Rb⁺, Cs⁺) on a strip of nitrocellulose. Ignition of one end of a nitrocellulose strip initiated propagation of a flame-front (at $T \approx 1000^\circ\text{C}$) at 2–3 cm/s. As this moving hot zone reached each spot containing added metal ions, it caused the emission of light at wavelengths characteristic of the thermal emission of the corresponding atomic species. The pattern of emissive salts, ordered in space, therefore, became a sequence of pulses of light at characteristic wavelengths, ordered in time. We have optimized infofuses to transmit messages using wavelengths in the near-infrared ($75 \text{ nm} < \lambda < 9 \text{ nm}$), and the total maximal power of each pulse of an infofuse was $\sim 1 \text{ mW}$. Therefore, the infofuse can weigh up to 10 g and fulfill the power density requirement. Using the 3 IR emitters (K, Rb, Cs), two consecutive pulses of light (49 unique combinations) are enough to encode the selected set of characters. We have demonstrated the transmission rate of characters (CTR) of 10–11 Hz using inkjet printing (with a desktop inkjet printer) using these experimental parameters.

The infofuses fabricated according to this design demonstrated the principle of a successful strategy for coupling chemistry with the encoding and transmitting of chemical information, but suffered from a number of weaknesses.. Two were of primary concern to us: i) When the flame-front of nitrocellulose infofuses with dimensions we used (1–3 mm wide, ca. 100 mm thick) came close ($< 1\text{--}2 \text{ mm}$) to any solid surface, their rate of propagation decreased, and the flame frequently extinguished. ii) The rapid propagation of the flame-front (ca. 3 cm/s) precluded times of transmission longer than about 1 min (an infofuse on which the flame propagated at this rate would require a length of 2.6 km to transmit continuous or repetitive messages for 24 h).

In Phase II, we developed a new experimental platform for infofuses that addresses these weaknesses by using a “dualspeed” arrangement, in which a fuse that burns slowly and continuously (a “SlowFuse”) and that does not transmit information, intermittently ignites fuses (strips of nitrocellulose) that burn quickly and transmit information (“FastFuses”). This design enables us to repeat a message, or transmit different messages, periodically. The design we use here—in which FastFuses are supported on a thermally insulating support (fiberglass), or separated from the surface by some other methods (e.g., crimping)—also increases the mechanical and thermal stability of the devices, and allows them to be used in a range of

orientations. For two-speed configuration of fuses, we glued FastFuses to the SlowFuse by applying a solution (5% w/v) of nitrocellulose in acetone and allowing the solvent to evaporate. Small quantities (<10 mg) of flammable solids at the junction of the two fuses allowed the SlowFuse to ignite the FastFuses. To demonstrate using this two-fuse system to transmit information, we appended seven FastFuses to a SlowFuse. Each FastFuse was encoded with its distance from the beginning of the SlowFuse, i.e., the FastFuse that was 1.5 feet (ca. 45 cm) from where the SlowFuse was ignited transmitted the message “1.5 FEET”. For this two-speed fuse on a glass wool, the five-foot long SlowFuse did not extinguish until it burned completely (after 45 min).

We also successfully developed and implemented a new error-correction scheme that is tailored for the particular noise that is observed for the infofuse. Transmission of any complex signal will involve noise in a variety of ways: insertion of unintended signal peaks due to non-uniform propagation of the flame front or imperfection of the application of the salt, as well as imperfections in the simultaneity of peaks when using combinations of the salts. In order to increase the reliability of the message while reducing the redundancy included in the signal, we incorporated a multi-layered sequence of check bits that allow us to recover the message in the presence of noise. Our approach is robust while taking relatively few check bits (good recovery was observed for a 14 bit signal sending a 10 bit message, with under 30% of the signal comprising error correction). We have also implemented the error correction on an iPod, which is able to perform the correction accurately and rapidly.

In the no-cost extension, we successfully increased the maximal frequency that information is transferred by a factor of two over the two-pulse scheme, and also reduced errors in the detected signal by encoding each character with a single optical pulse. We designed and implemented two new schemes: i) a scheme that is binary (0,1) in the intensities of light emitted from six (Li, K, Rb, Cs, Sr, Ca) thermal emitters; ii) a scheme that is binary and ternary (0, 1, 2) in the intensities of light emitted from four (Li, K, Rb, Cs) thermal emitters. These approaches improved previously demonstrated systems of “infoFuse”. By employing a binary system in intensity using six different thermally emissive salts or binary and ternary system in intensity using four different thermally emissive salts, we can encode and transmit alphanumeric information with individual optical pulses. New encoding schemes allow us to improve the density of the information with lower error rate than previously described systems

Droplet Laser

We used 3 dyes lasing at 3 different wavelengths (Rhodamine 590, 600 nm; Rhodamine 640, 650 nm; Cresyl violet 670, Oxazine 720, LDS821). A character is represented by 4 droplets, each droplet with 3 possible lasing wavelengths. The number of characters represented is therefore $3^4 = 81$. To encode a 60-character message, we use $60 \times 4 = 240$ droplets. Different orders, which we could arrange by using dielectric sorting, of dye droplets represent different characters. The orders of dye droplets are arranged by using dielectrophoretic sorting. We have demonstrated > 1000 droplets/sec with which we met the milestone of a character transmission rate greater than 10 Hz. Energy capacity of the droplet laser system is 229 mW/g.

Bubble Shutter

Research on bubble shutter has been focused on finding other potential uses for the bubble shutter system. We began this phase by looking to improve the functionality of the bubble shutter in two ways: i) increasing the amount of information per unit length of the channel (i.e. information density) by manipulating other variables related to the droplets, light source, mask, and the detector, ii) by using the bubble shutter to characterize the size and velocity of droplets, which could be more generally useful in microfluidics.

We previously viewed the bubble shutter as a digital device: in the simplest case, when a droplet was above a window in the mask, the detector measured either the presence or absence of a signal (i.e. a binary signal, either 0 or 1). We extended the binary signal to a base-N signal by introducing variable sizes and shapes of windows on the mask, and analyzing the resultant intensity responses as a function of time. We further began initial demonstrations on how information about the shape and velocity of the droplet can be used to achieve analog transmission. Additional orthogonal properties of the system, such as the polarization or spacing between the windows, can also be used to increase the information density.

Our work on using the droplet shutter-based system to measure the size of the droplets would provide an alternative to current methods of sizing droplets for microfluidic devices that rely on image analysis. Such systems necessitate a costly, high-speed camera and are difficult to implement in real-time or for experiments of long duration. On the other hand, our droplet shutter doesn't require a CCD array and the measurement can be easily adapted to the design of

existing microfluidic devices. Furthermore, it can measure the multiple droplets simultaneously for a long period time.

Summary of milestones for Phase I, II and no-cost extension

Phase I – Proposed	Result
1. Demonstrate a scheme for the modulated chemical encoding of the alphanumeric character set consisting of the letters A-Z, the numbers 0-9, and at least two “space” characters.	Achieved, using all three infochemical systems
2. Demonstrate a breadboard replicator device that permits the user to input a 60-character alphanumeric message, translates it into a set of modulated chemistries, embeds these chemistries into a disposable substrate (the transmitter), and ejects the substrate for deployment.	As of yet, we still manually generate transmitters.
3. Demonstrate the capability to construct a 60-character message, convert it to a NIR-SWIR optical signal, repetitively transmit the signal to a receiver for a duration of > 1 hr with a CTR (character transmission rate) of > 10 Hz, and decode the signal to recover the message. The light-emitting components must have an energy capacity of > 100 μ W/g.	Achieved: - 1 hour duration - 10 Hz CTR - decoder software - energy capacity

Phase II – Proposed	Result
1. Development of a prototype Chemical Communications device with the form factor of a PDA or cell-phone;	Developed a decoder software with an error-correction ability (iPhone app). Detector is still telescopic.
2. Development of a prototype disposable transmitter with the form factor of a sheet of paper with an adhesive backing;	Achieved using infofuse
3. Demonstration that the Chemical Communications system that meets or exceeds the performance metrics provided for Phase I will now repetitively transmit the signal to a receiver for at least 100 hours.	Possible with InfoFuse (6.7 feet required per hour) and droplet laser/shutter (these systems operate indefinitely)

No-Cost Extension – Proposed	Result
1. Improvement of the density of the information with lower error rate than previously infoFuse system.	Achieved using single-pulse encoding schemes with infoFuse

Tufts University

Infochemistry

For the infochemistry project, our laboratory was responsible for developing an instrument/detector to observe the emission signals from the burning fuse developed at Harvard in the Whitesides Laboratory. We developed multiple systems for the project.

Initial Detector System Screening

We developed and tested a number of different detection platforms to identify pulses of NIR radiation. We concentrated on detection for the infuse, but the methods are transferable to other parts of the chemical communications project. These platforms are summarized in Table 1, and four of the platforms are shown in Figure 1.

Table 1. Summary of detection systems and capabilities.

Detection Setup	Distance tested	Wavelength Range	Wavelength resolution (nm)	Acquisition type	Spatial Resolution (Y/N)
2 convex lenses, UV-vis spectrometer (fig. 1A)	3 m	350-1050 nm	3	Simultaneous	N
IR viewer, camera	1 m	<1300 nm	N/A	Simultaneous	Y
monochromator, IR viewer, camera (fig. 1C)	40 m (LED)	<1300 nm	3	Scanning	Y
monochromator, PbS detector	1 m	1 – 2.5 μ m	4	Scanning	N
convex lens, concave lens, UV-vis spectrometer (fig. 1B)	12 m	350-1050 nm	3	Simultaneous	N
convex lenses, filters, photodiodes (fig. 1D)	Not tested	3 fixed wavelength	~5 nm (filter dependent)	Simultaneous	N
convex lens, concave lens, InGaAs spectrometer	Not tested	900 – 1700 nm	2 nm	Simultaneous	N

In some cases, we designed the light gathering lenses to maximize collection efficiency while minimizing position sensitivity. While the position of the flame front will likely be negligible in the final system, intensity variation due to position can be significant for testing emitters only a few meters away. Some systems use a compact UV-Vis spectrometer to capture an entire spectrum from 350 nm to 1050 nm at ~ 100 Hz. Using this detector we first decoded a patterned fuse from 12 m away with the room lights on. Other systems capture monochromatic images that can identify the location of IR sources, but are not practical for rapid multi-wavelength imaging. The system we settled on contained three notch filters and three detectors from which data can be collected simultaneously and analyzed by an external circuit.

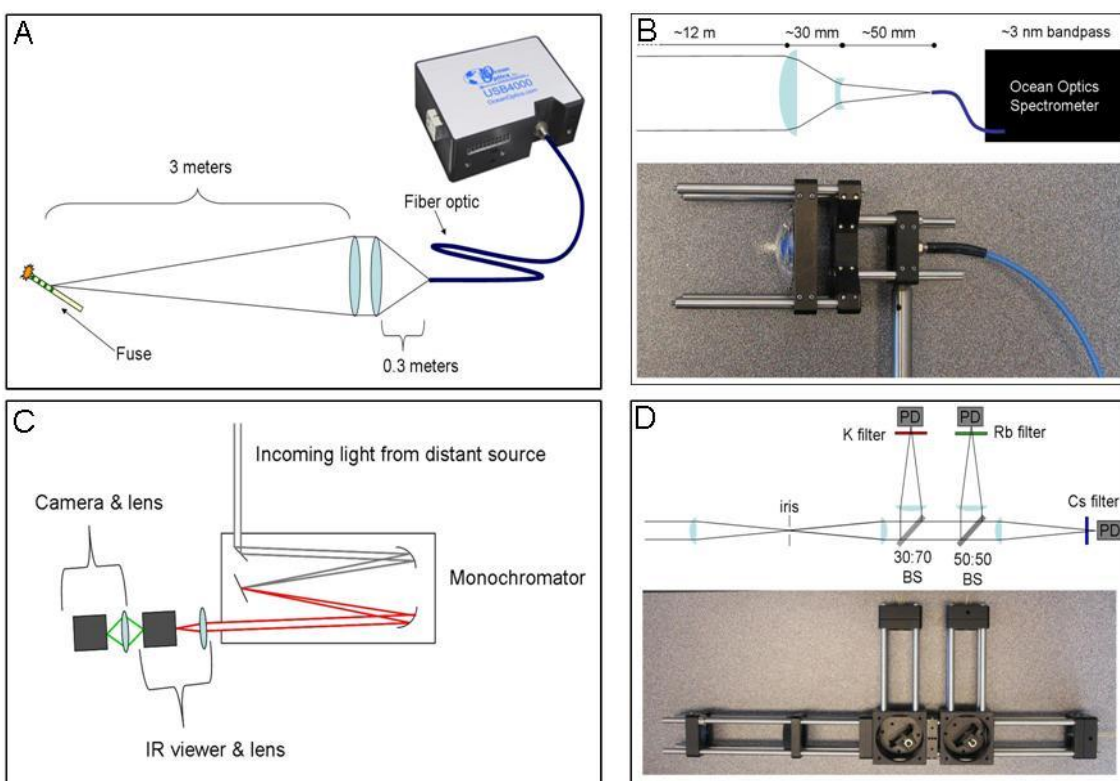


Figure 1. (A) Detection setup for a fuse a few meters away with minor sensitivity to position. (B) Longer range setup, used to detect NIR pulses from over 10 m away with room lights on. (C) Monochromator and IR viewer setup used to capture monochromatic IR images from distances over 40 m. (D) Filter based platform for the detection of three different atomic species.

1st Generation Filter-Based System

The first generation of the filter-based system uses telescope-style optics to collect the emission from a distant fuse. The incoming light is split into four channels. The first channel carries visible light to an eyepiece or a camera so that the system can be easily aimed at the fuse. The NIR light is split amongst the remaining three channels, with each of these channels corresponding to a different element's (K, Rb, or Cs) emission. The detectors are extremely sensitive in the NIR and each has a very narrow (1 nm FWHM) bandpass filter to exclude background light. Using this system we were able to detect atomic emission from a fuse from 300 m away.

2nd Generation Filter-Based System

We then constructed the next generation detection system shown below.

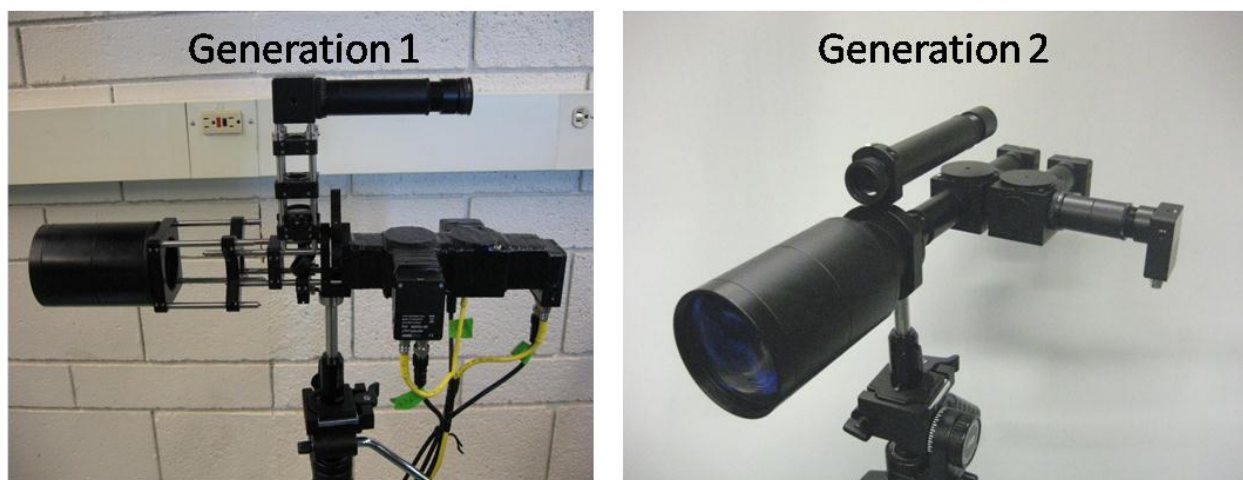


Figure 2. Photograph of the 1st and 2nd generation filter-based systems.

We constructed a 2nd generation detection system. This system has several advantages over the previous system: 1) it is completely enclosed, which will reduce stray light and 2) each detector has an adjustable entrance pupil allowing each channel to be attenuated individually, 3) the dichroic filters have sharper cutoffs to maximize transmission and reflection of the appropriate wavelengths, 4) this system has a CCD camera on the scope allowing the user to record an image of where the signal is coming from. A photograph and schematic of the second-generation detector is shown in Figure 3.

The collection lens (200 mm FL, 3" diameter lens) is the same as the 1st generation, but the lenses before the detectors have a longer focal length. This modification made it easier to position the detector at the focal point because these lenses have a longer depth of focus. Since the system is enclosed using tubes, the detector position can be optimized in real time while aimed at a target. This method was not possible with the old system, which used rails instead of tubes. The rails were covered with blackout cloth that prevented access to the detector.

We performed a side-by-side comparison of the new and old systems. The new system performs significantly better on the potassium and rubidium channels and slightly better for cesium. This performance increase is shown in Figures 4 and 5 below.

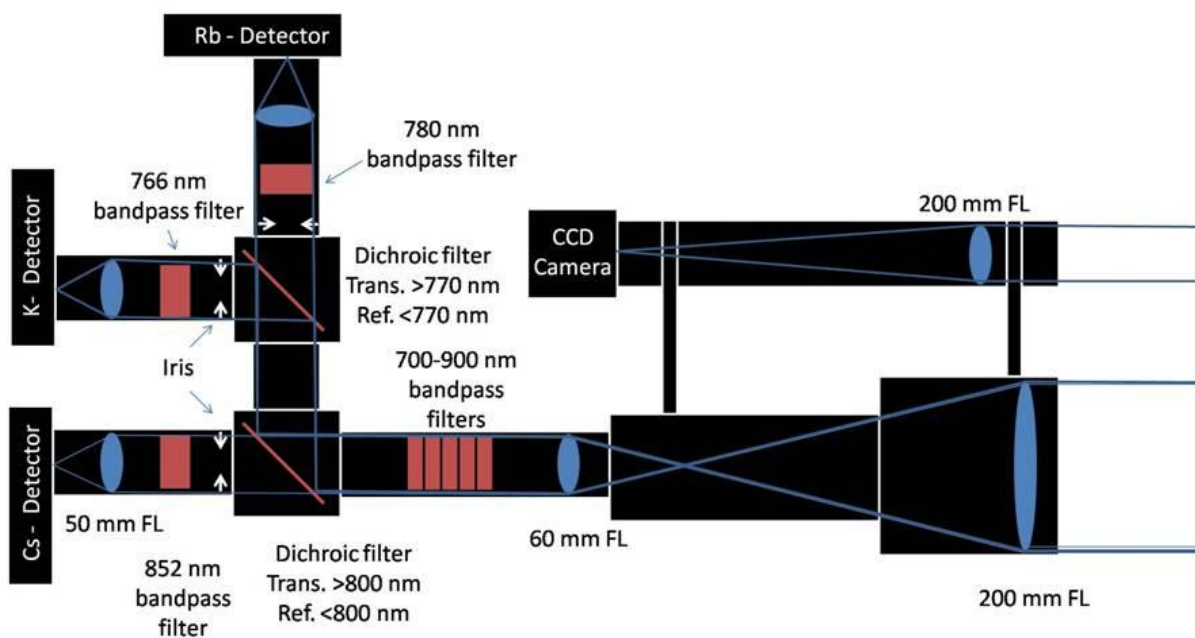
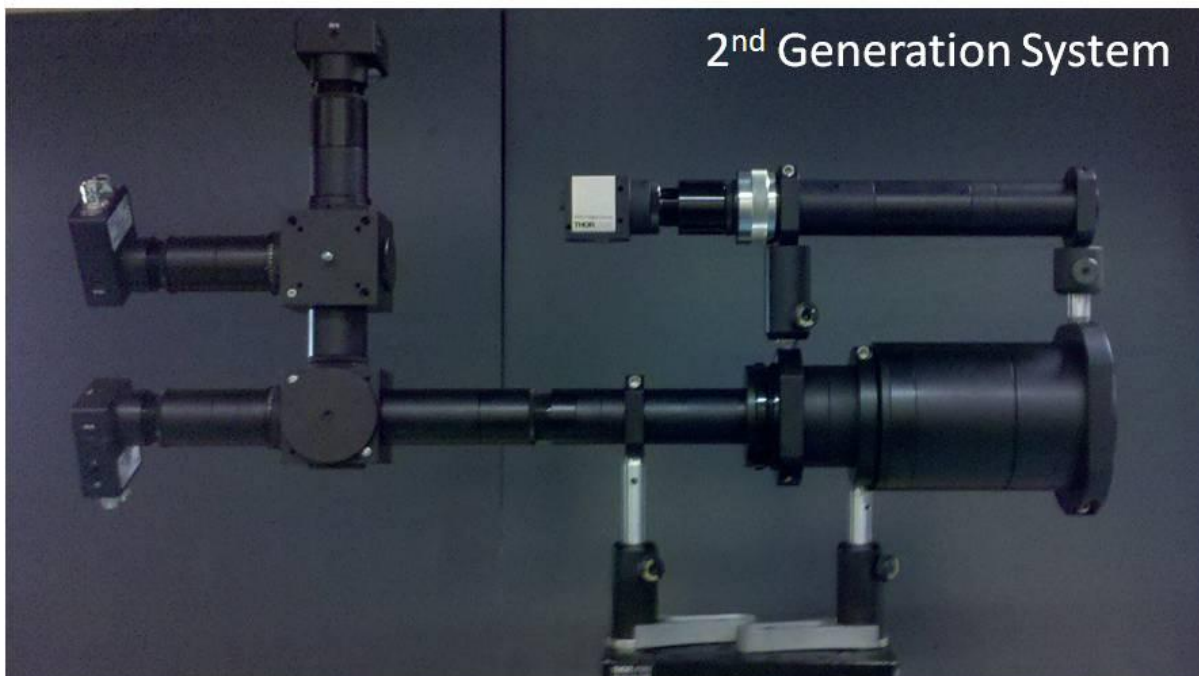


Figure 3. Top: Photo of 2nd generation detection system. Bottom: schematic showing lenses in blue and filters in red. The blue rays are traced coming from infinity.

Side by Side Comparison at 600 m

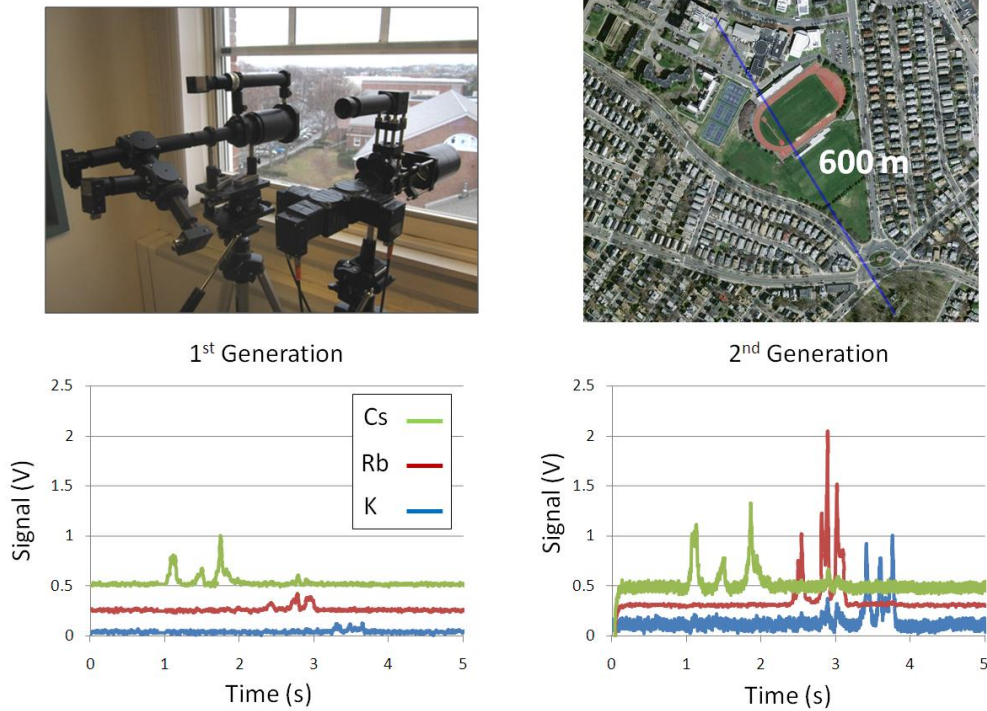


Figure 4. Side by side comparison of 1st and 2nd generation detection systems. The fuse data were collected at night from 600 m away

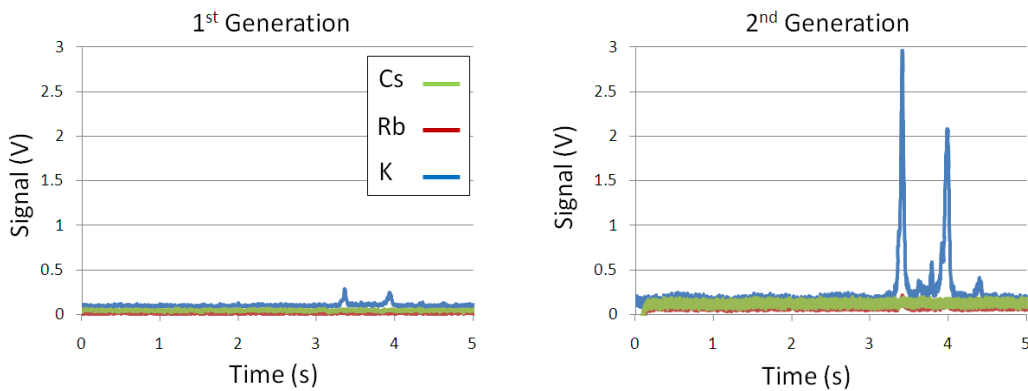


Figure 5. These data are from a fuse spotted with two spots of K and burned 600 m away. The fuse was submerged under water for 10 s before burning. These results show the improvement in the 2nd generation detection system and they also show that the fuse still gives a strong signal even after being held under water.

We characterized the 2nd generation detection system by performing long range (~600m) measurements to determine the field of view of the telescope. The system has a detection angle of 1°, which corresponds to approximately a 100:1 ratio between the distance and the field of view. That is, if the fuse is 100 m away then it can be detected in a 1 m window.

We also tested the effect of direct sunlight on the telescope. Full afternoon sunlight was shining on the telescope while we picked up signal from a fuse 80 m away (Figure 6). The filters before each detector blocked most of the sunlight; adjustable irises before each detector were opened such that the background level was ~4 V. The fuse signal was easily detectable as shown below.

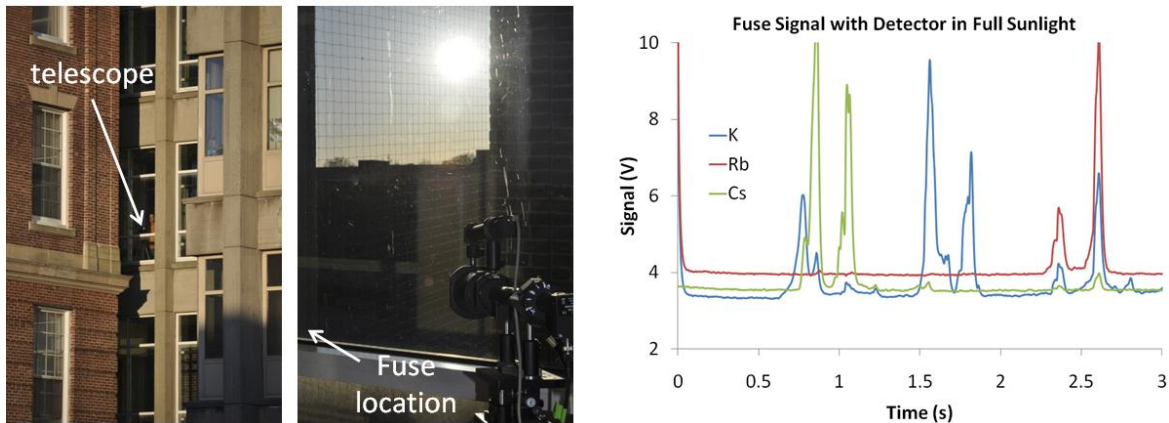


Figure 6. The pictures on the left show the telescopic detection system in the window in full afternoon sunlight. The data shown on the right are from a fuse 80 m away.

1st Generation Portable Message Decoding System

A portable system was designed to detect an infrared signal pulse train and display it on a LCD module. The system block diagram is shown below in Figure 7.

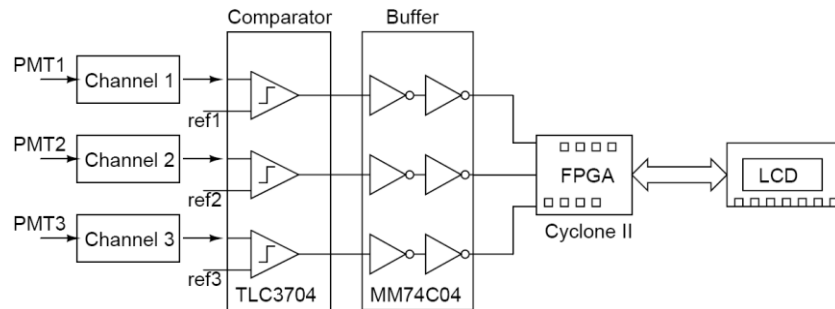


Figure 7. Block diagram of portable detection system

A customized PCB was designed and implemented to perform as analog front end with basic signal processing functions. The input infrared signals are detected and amplified by three high sensitivity photoreceivers (PMT1 ~ PMT3), which are interfaced with a three-channel voltage comparator via Channel 1 ~ Channel 3 adaptors. The threshold voltages ref 1 ~ ref 3 of the comparator can be independently adjusted to compensate for different spectral responses from the three photoreceivers. The digital outputs of the comparator are scaled by a voltage buffer and then sent to an off-board FPGA system. In this 1st generation system, we have used an FPGA evaluation board (ALTERA DEII) for time-efficient implementation. In the 2nd generation system we will integrate an FPGA chip on the same PCB for further reduced system size and power consumption. The digital outputs from PCB are operated under a set of simple XOR Boolean algorithms and the results are sent to a LCD module, whose display operation is in turn controlled by the FPGA board. The following picture shows the actual hardware implementation.

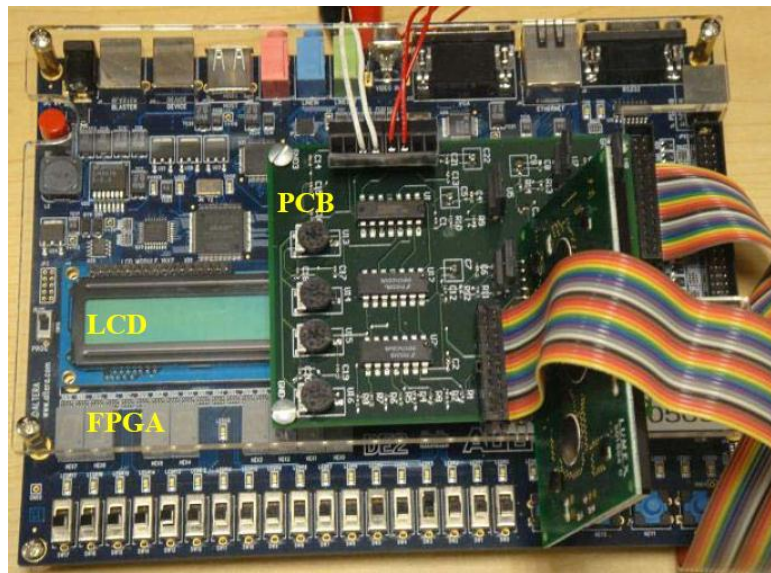


Figure 8. 1st Generation portable Infofuse detection system

The system is powered by a 15V power supply. Such high power consumption is due to the fact that the output from the highly sensitive photoreceiver has a 10V voltage swing. A high sensitivity photoreceiver is necessary in our system to detect weak infrared signals in the presence of large background noise when the fuse is far away. The sampling frequency of our portable device is 400Hz, which is well above the Nyquist rate of data transmission.

The portable device has been integrated with the optical detection system, and proof-of-concept experiments were performed using both flashing LEDs and burning fuels with a data rate of around 1Hz. The following figure shows the experimental setup for the portable detection system.

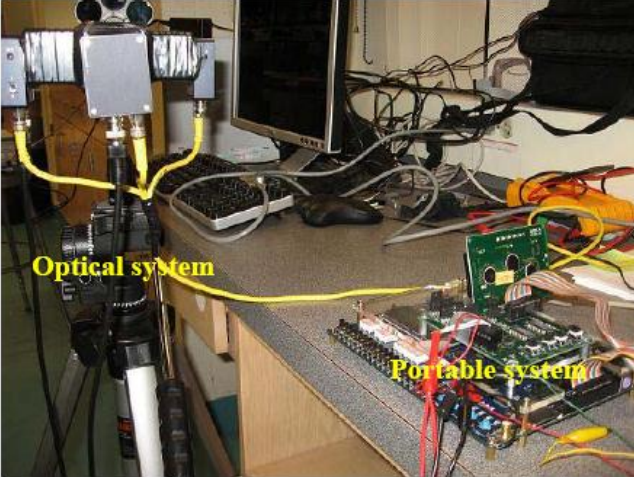


Figure 9. Experiment setup for real-time display of digital data

During the first experiment, two flashing LEDs were continuously switched on and off at 1Hz. One LED was used as the trigger source while the other LED was used as the signal source. A total of 16 message bits, corresponding to eight signal pulses, were recorded and displayed on the LCD, as shown in Figure 10.



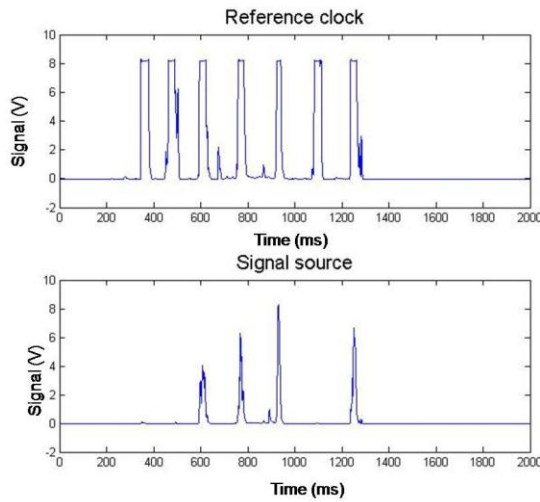
Figure 10. Detection of continuously flashing LCD—eight pulses were detected (10, 10, 10, 10, 10, 10, 10, 10) and a total of sixteen message bits were recorded and displayed.

During the second experiment, the signal LED source was blocked manually in the middle of the series. The results are shown in Figure 11.



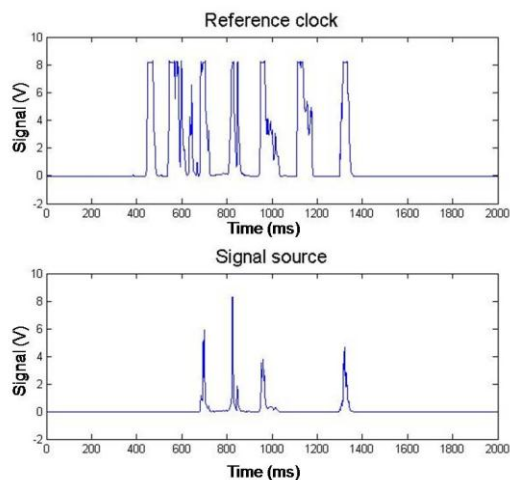
Figure 11. The middle of the message was blocked, resulting in three pulses (10, 10, 10), followed by six zeros (middle of the message that is blocked), and two pulses at the end (10, 10).

We measured emission from patterned fuses using the signal processing circuit described in the last report. This circuit has an adjustable threshold that is used to determine the occurrence of a pulse of light on the detector. The system is similar to lock-in detection in that the circuit checks the signal intensity following a clock pulse. For the moment, the clock is patterned Cs and the signal is patterned Rb. In the 2nd generation, any of the three metals (K, Rb, or Cs) can be the clock source, and we will not lose a detection channel by having it as a designated clock channel. The circuit reports “00” if there is no signal present when the clock pulse occurs and reports “01” if there is a signal pulse emitted with the clock pulse. The two figures below show the full data recorded with LabView and the processed data output from the signal processing circuit.



Portable device:
 0000010101000100
 (2 clock, 3 signal, 1
 clock, 1 signal)

Figure 12. The reference clock data show 7 Cs pulses in ~1 s. The signal source shows 4 Rb pulses emitted with the 3rd, 4th, 5th, and 7th clock pulses. The zeros and ones shown on the right are from the signal processing circuit output using a threshold of 1 V for the signal.



Portable device:
000000001000100
False detection due to
noisy reference clock

Figure 13. The reference clock data show 7 Cs pulses in ~1 s. The signal source shows 4 Rb pulses emitted with the 3rd, 4th, 5th, and 7th clock pulses. The zeros and ones shown on the right are from the signal processing circuit output using a threshold of 1 V for the signal. Since the clock pulses were noisy, the processed signal is incorrect (the zeros and ones should have looked like they do in fig. 1)

2nd Generation Portable Message Decoding System

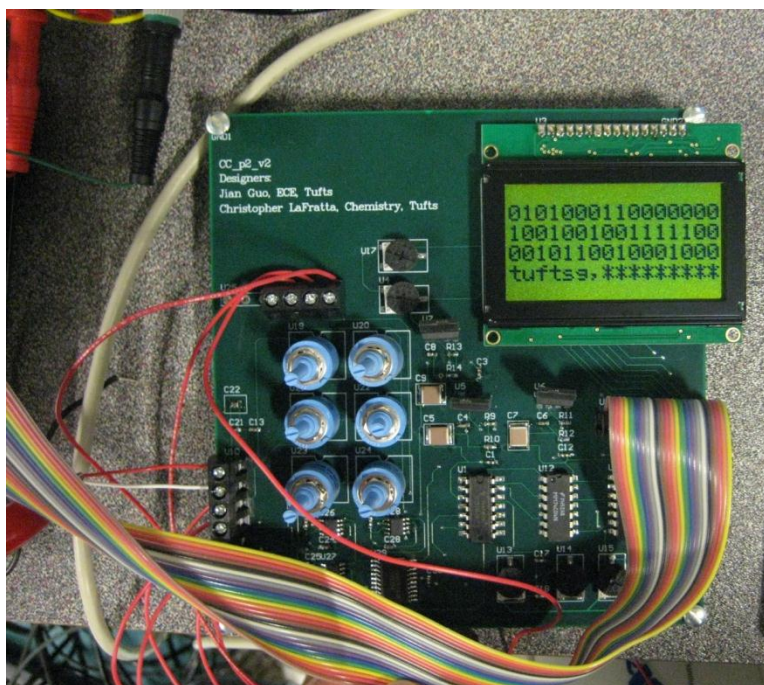


Figure 14. Photograph of the 2nd generation message decoding system.

We improved our detection circuit so that it no longer uses one of the optical channels as a clock for triggering. The circuit is now triggered off any of the three channels and records a pulse whenever the signal crosses the threshold for each channel. The thresholds for each channel are independent. When a pulse is detected on one channel, the other two channels are queried to check if they also received a pulse. This signal is put through a low pass filter to smooth spikes in the fuse emission and the results are displayed as 0's and 1's for each channel. The digital data are also translated into English using a look up table. The message in Figure 14 reads "tuftsg," which is the message "tufts" plus the check bits, which describe the message and translate to "g.". This circuit is efficient in terms of memory in that it only records observed pulses. If there is a long delay between pulses, the circuit does not record anything.

The data recorded by this system may not necessarily be the signal intended by the sender—sometimes errors occur from fuses that burn inconsistently. An error correction algorithm was implemented by the Harvard team and was shown to be effective during our experiments. Figure 15 shows a typical insertion error that can result from a flame that flares up momentarily causing two peaks instead of one. Insertion errors and permutation errors can both be corrected using the detection system and the algorithm, as shown in Figure 16.

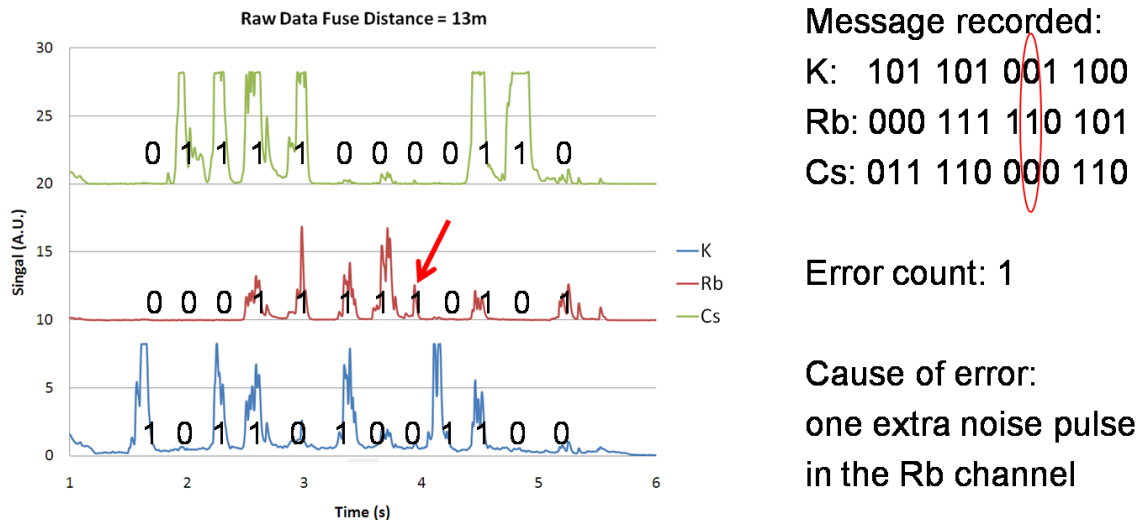


Figure 15. The analog data recorded for each channel are overlaid with the digital data recorded by the detection circuit. The red arrow indicates a spurious noise spike, which was recorded as an extra peak in the digitized data. This type of error is correctable using the error correction algorithm for message encoding that uses check bits.

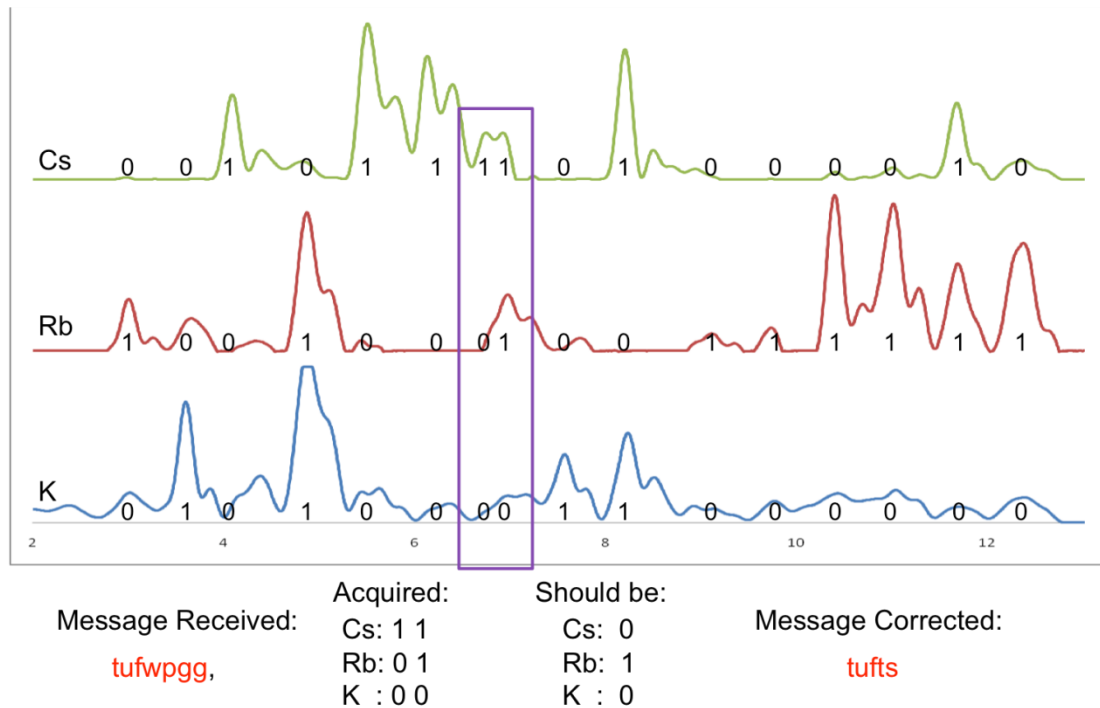


Figure 16. Filtered data recorded by the decoding system. Note that the received message contained an error, outlined in the purple box, which was corrected using the check bit algorithm. This error correction was not hardwired into the decoding system and could be performed using another computer such as an iPhone.

Conclusion

After screening several different detection system options we built a filter-based system, which allows for long distance (~600 m) detection of the infofuse signal. This system was optimized in the second generation and combined with an external processor that could digitize and translate the received pulses in real time. These translated messages could then quickly be checked with the error correction algorithm to check for possible other intended messages.

Atomic Emission Beacons

As a spinoff of the Infochemistry project, we investigated “canned heat” (a.k.a. Sterno) for its potential use as an atomic emission beacon. As demonstrated with the infofuse, thermally excited atomic emission is detectable over large distances, despite low intensity, because of its narrow spectral line width. We hypothesized that if we could dope a conventional heat source then we may be able to make a continuous, isotropic, spectrally-narrow emission source that is chemically powered, portable, and reliable. This light source could be useful as a beacon for long duration continuous emission. It could be used for Morse code signaling and has the advantage of being isotropic and invisible.

We made the fuel source by combining a saturated solution of calcium acetate with ethanol. This mixture forms a gel that burns steadily for several minutes or hours depending on the quantity. We then stirred in salts of K, Rb, and Cs. The emission spectrum of the doped alcohol flame is shown below.

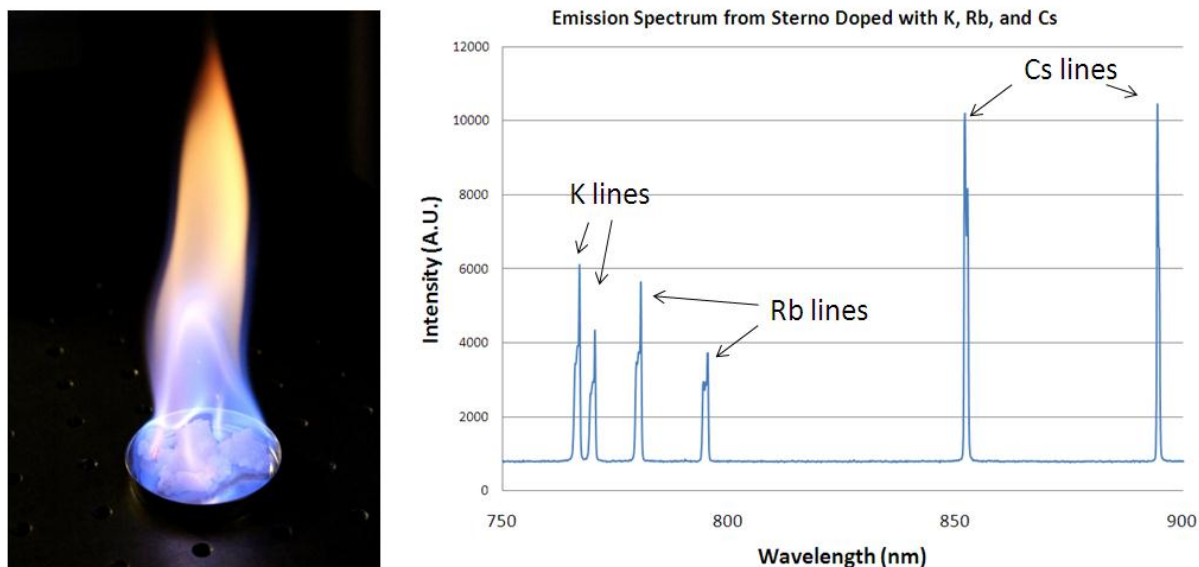


Figure 17. The picture on the left shows homemade Sterno that has been doped with K, Rb, and Cs salts. The spectrum on the right shows the sharp emission lines from these elements.

The flame looks visible in the photo but under normal lighting conditions it is nearly invisible. It takes on a slight purple tint when doped with the alkali metals, but it is not very luminescent in the visible at all. We collected data from doped alcohol burned 200 m away at night. Even with

only 1 mg of Cs salt, the signal was well above background. As shown in figure 18, we saw higher signals with increasing concentration.

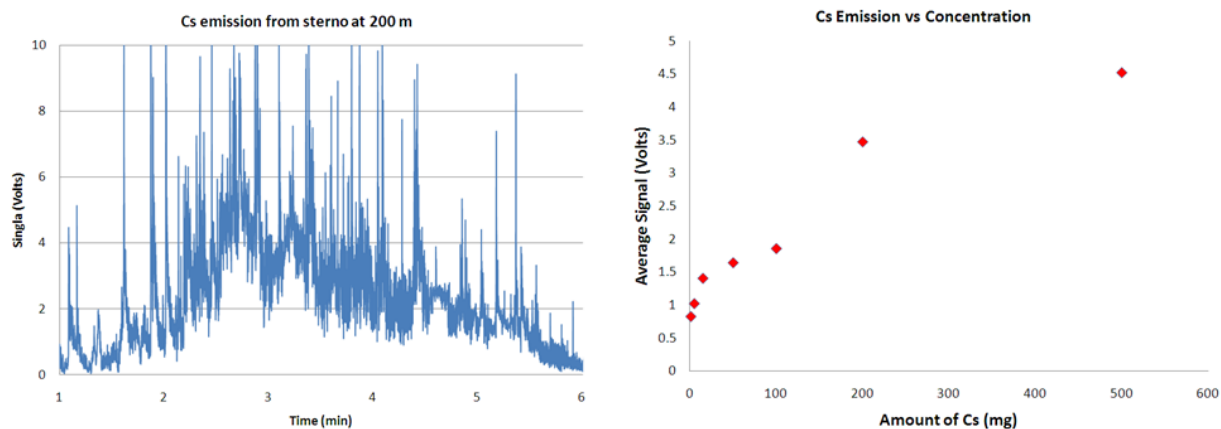


Figure 18. (Left) Graph of Cs emission from alcohol doped with 200 mg of CsNO₃ at a distance of 200 m. (Right) Concentration study comparing the intensity as a function of the amount of Cs added to the sterno. Each point is the average value over several minutes of burning.

We tested the distance dependence of the signal (Figure 19.) using Cs at Long Beach in Nahant, MA (Figure 20). The signal could be detected over 1.5 km away. Note that the closest data point seems to plateau in intensity, because the detector was frequently saturating at this distance. If that closest point is ignored, the remaining data fit the expected inverse-square law with an R²-value of 0.95.

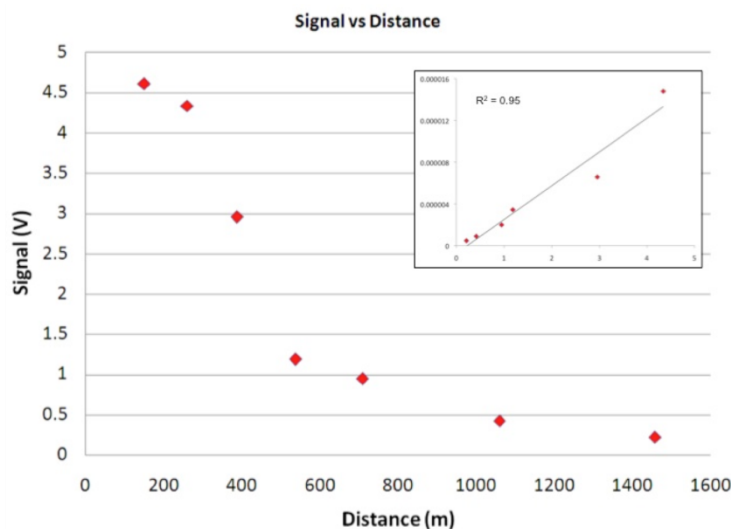


Figure 19. Plot of signal intensity vs. distance for a sample containing 100 mg of CsNO₃. The inset shows the same data plotted vs the reciprocal of distance squared.

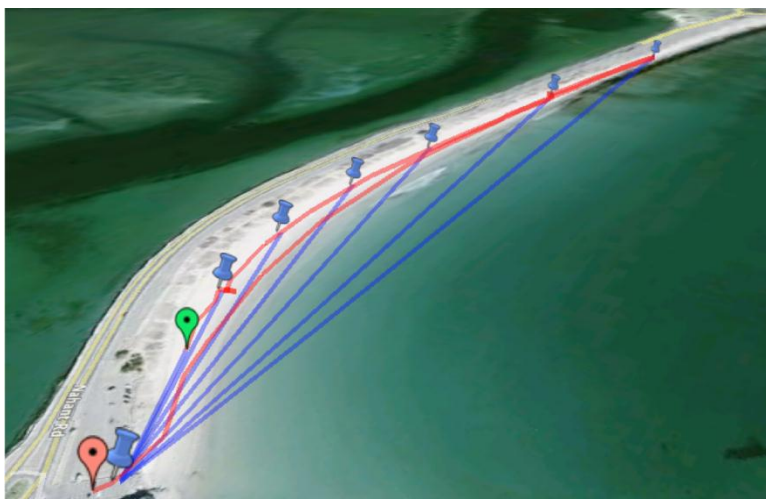


Figure 20. Google Earth image of Long Beach, Nahant, MA. The red marker indicates the position of the detector and the blue markers were locations where the message was transmitted.

Infobiology (taken from PNAS 2011, 108(40), 16510-4.)

The intrinsic high information content and information flow in biological systems has the potential to be used to translate non biological genetically encoded information into an easily read phenotypic signal. In this context, genetically engineered systems are of particular utility because they enable exquisite control of both genotype and phenotype (1). Here we describe the use of *living organisms* as the carriers of encoded messages. Phenotypic features have previously been used as cipher keys for the identification of individuals. Biometric ciphers, such as fingerprint, iris, and retinal scans, are examples of ways in which the unique phenotypic characteristics of individuals can be used to control access to facilities or data (2). Although biometrics have found their way into “real-world” applications, biometric ciphers only function as cipher keys and do not play a role in the storage, transmission, or encoding of data. Examples of information embedded in biological systems include the insertion of synthetic data-encoding DNA (non-protein coding) for trademark and watermarking purpose (3, 4) and for long-term information storage (5-8). Although such systems seem convenient for high-density applications of data storage, decoding high density information from non-protein coding DNA requires sophisticated sequencing capabilities for data readout.

We have previously employed chemical methods for encoding, storing, and sending information using a method dubbed “InfoChemistry” (9-11). In this paper, we develop a new way of

transmitting information called InfoBiology that uses living organisms for these functions. This work constitutes an initial step to combine biochemical signals with information theory to produce an alphanumeric message (Figure 1a).

We use cytosolic expression of fluorescent proteins (FPs) in *E. coli* as a phenotypic marker to encode messages. The levels and timing of expression of proteins can be controlled by several biological inputs (or bio-ciphers), e.g. bacterial strain, type of vector (high- or low-copy origin of replication), growth medium, promoter site, and maturation time of fluorescent proteins. For our proof-of-principle experiments, we prepared different strains of *E. coli* that were engineered to express high-copy numbers of seven different FPs: GFPuv, AmCyan, ZsGreen, ZsYellow, mOrange, tdTomato and mCherry under control of the bacteriophage-T7 promoter (See S.I. for details). This series of FP encoding vectors contain the ampicillin-resistant gene as a selective marker. We used two different host strains of *E. coli* to express the FPs. First, we transformed BL21(DE3)pLysE *E. coli* cells with the series of FP encoding vectors mentioned above. BL21(DE3)pLysE cells contain the gene encoding for T7 RNA polymerase under the control of the *lacUV5* promoter, allowing expression of T7 RNA polymerase to be induced by isopropyl β -D-1-thiogalactopyranoside (IPTG). The BL21 strains yield an “on-demand” system as these strains require induction to develop a potential message properly. Next, TOP10 *E. coli* cells were transformed with the same FP encoding vectors to generate an “induction free” system. TOP10 cells do not contain the gene encoding for T7 RNA polymerase and therefore are not sensitive to IPTG induction. TOP10 cells are, however, engineered to allow stable replication of high-copy number plasmids. The high concentration of the plasmid allows for a high background “leaky” expression of the FPs, which can easily be detected by fluorescence imaging after 48 h of incubation under ambient conditions (See Figure S1 S.I.).

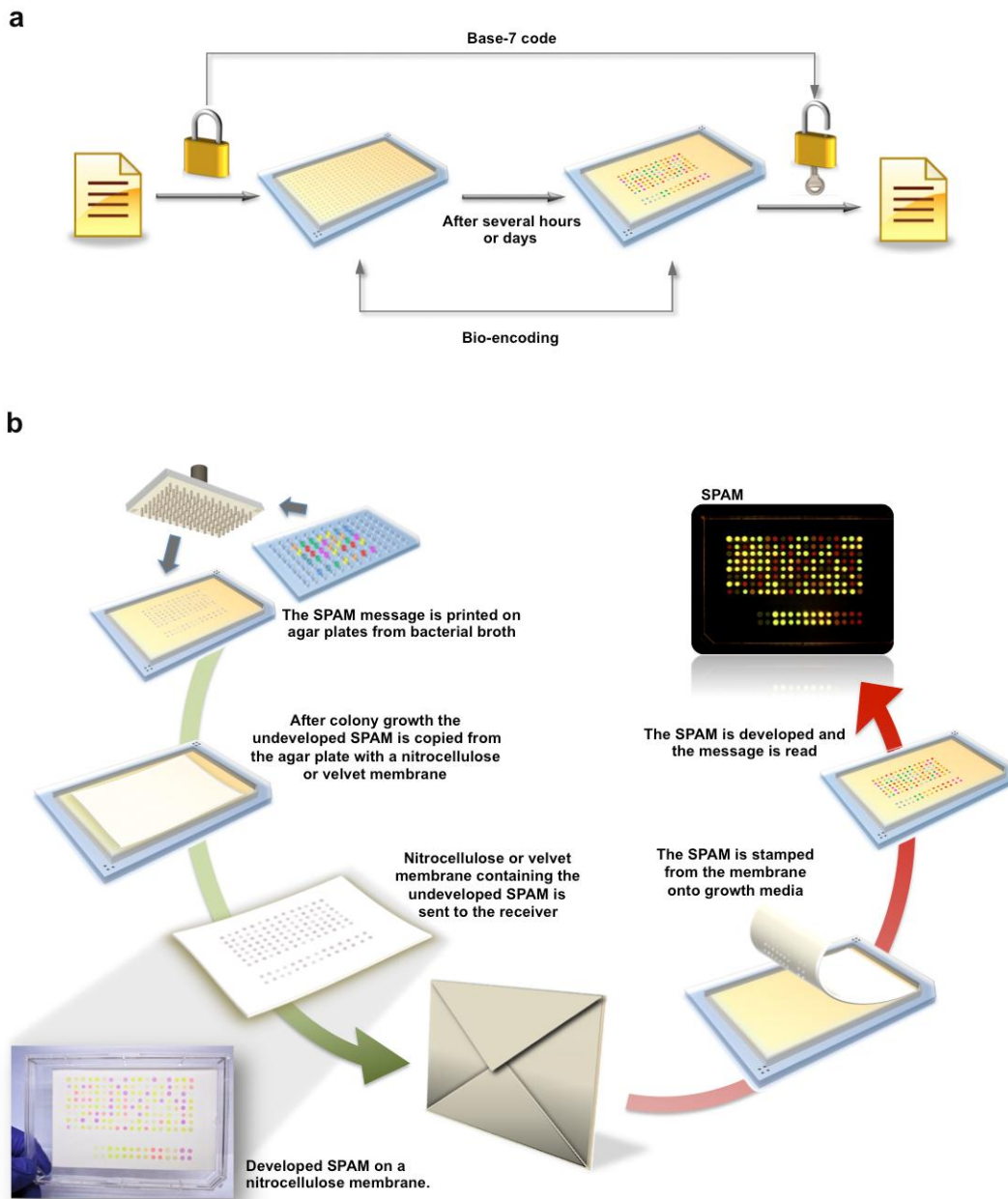


Figure 1. **a**, Schematic illustration of the information workflow in a bio-encoding system. The sender encodes the message using a septenary code. The SPAM (Steganography by Printed Arrays of Microbes) message is developed under pre-determined growth conditions and read out with a pre-determined set of excitation/emission wavelengths, which constitute the bio-cipher and photo-cipher keys, respectively. Finally, the receiver compares the output with a pre-determined code. **b**, Scheme showing the preparation and read-out of a SPAM. The green arrow follows the sender's actions to prepare a SPAM, while the red arrow follows the receiver's

actions to develop a SPAM. First, broth containing fluorescent bacteria is pipetted into a microtiter plate. Second, a multi-blot pin replicator is used to transfer a small volume of the broth from each well onto a target plate containing the appropriate growth media. After the undeveloped SPAM is grown, it can be transferred to a nitrocellulose or velvet membrane for delivery. The receiver stamps the SPAM onto an appropriate growth medium, develops the signal, and reads the SPAM message. Note that the “undeveloped” SPAM does not have a clear color read-out because protein expression has not yet been induced. For illustration, an image of a nitrocellulose membrane containing a “developed” SPAM is shown at bottom left.

Infobiological data can be organized in different ways to convey a message. In the case of the previously-reported infofuse (11), the spatially arrayed data along the infofuse resulted in a timed sequence of pulses of IR emission, which were then converted into a message. In the microorganism-based platform described here, we array the data in spatial domains to form a matrix of fluorescent colonies. To produce the SPAM, fluorescent bacterial strains are first grown in selective broth media and are then transferred to a source microtiter plate. Subsequently, a multi-blot pin replicator is used to transfer 0.1 μL of the bacterial broth onto target agar plates (Figure 1b). Alternatively, after growing the colonies on agar, a nitrocellulose or velvet transfer membrane can be used to harvest the message from the agar plate. After copying the array of colonies, the membrane containing the message can be used to regrow the message, e.g. in a different growth medium. Depending on the application or setting, the membranes have the potential to be used as a carrier to store and/or distribute messages that is more convenient than agar plates.

Given the photophysical properties of the FPs, the signal of each fluorescent protein can be different depending on which excitation light source and emission filters are used. For our proof-of-principle example, we imaged the array with a filter combination (photo-cipher: $\lambda_{\text{exc}}=470\text{nm}$; $\lambda_{\text{em}} > 535\text{nm}$) that gave the highest information density. Figure S3 (See S.I.) shows clustering of seven distinct microbial FP signals when plotting the green versus red channels of the color image of a SPAM. This information density allows for the data in the SPAMs to be encoded in a base-7 (septenary) encoding scheme (Figure 2a). Each character is encoded by a pair of two septenary digits for a total of 49 (7^2) alphanumeric characters. Figure 2b shows SPAM of 144

colonies encoding a message containing 70 characters: “this is a bioencoded message from the walt lab at tufts university 2011”.

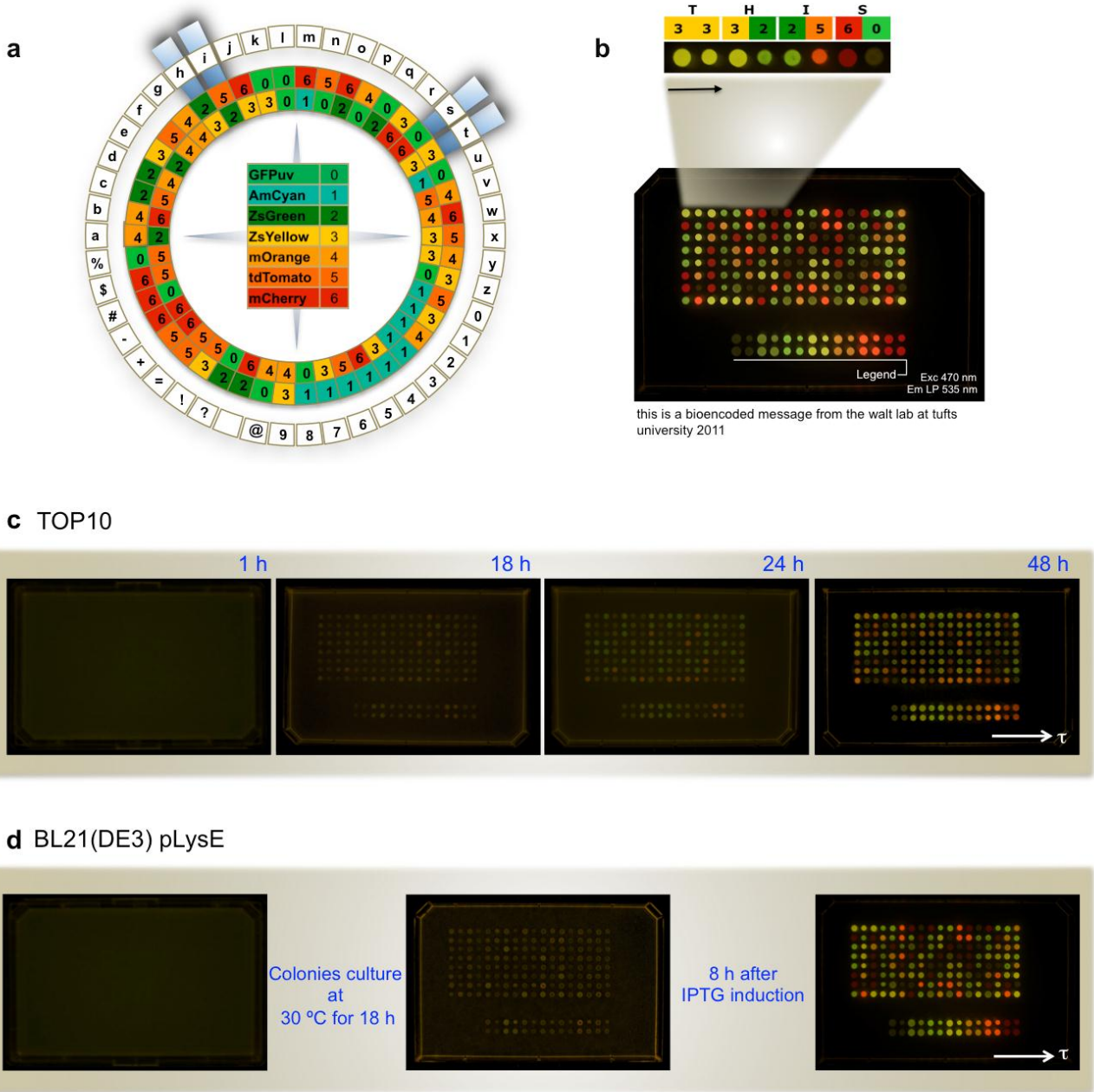


Figure 2. **a**, Septenary alphanumeric code. **b**, Fluorescence image of a SPAM consisting of 144 colonies, which encodes a message containing 72 characters. The message is read from left to right along lines that read top to bottom. The message reads “this is a bioencoded message from the walt lab at tufts university 2011”. **c**, Fluorescence images of TOP10 fluorescent strains

showing an array of colonies developed in approximately two days at room temperature. **d**, Fluorescence images of BL21(DE3)pLysE fluorescent strains showing that after growth of colonies, the FP expression can be induced by IPTG. Maturation of FPs takes approximately 8 h.

As mentioned, TOP10 and BL21 cells were transformed to produce systems for delayed-release and an “on-demand” delivery of messages, respectively. Figure 2c shows the timeline of an array of TOP10 fluorescent colonies growing at room temperature. Even though background leakage of the FP’s expression is evident after 18h, the signal intensity remains very low; at this time, fluorescent identification of the FPs is difficult. After 48h, the signal is strong enough for the message to be decoded. Figure 2d shows that in the case of BL21, the fluorescent bacterial strains also show some basal level of FP expression, but it is still difficult to correctly identify the FP’s emission signal. After IPTG induction, over-expression of the FPs takes place, but the message does not fully develop until after approximately 8 hours. This feature is due to the intrinsic clock associated with the fluorescent protein maturation time, which varies from protein to protein ([12](#)). Although there is delay for the “on-demand” system to deliver the message, the receiver can trigger the development of the message in a controlled manner using IPTG induction. It is worth noting that there are FP mutants capable of changing their emission properties over time ([13](#), [14](#)). These mutants would add an inherent security measure by self-deleting the message as it develops; similar to the way the Mission Impossible recording self-destructed.

One of the most useful features of this data storage/encoding system is the possibility of using selection markers as cipher keys to develop the correct message. Selection markers are genes that are introduced to an organism in order to provide a method of artificial selection when the organism is grown in a particular medium. Selection markers are commonly used as an indicator for the success of DNA transfection. One commonly used selection marker in bacteria confers antibiotic resistance to the cell. In order to demonstrate the possibility of using antibiotic resistance as a cipher key, all seven FP genes were cloned into kanamycin-resistant expression vectors containing a T7 promoter. Figure 3 shows a message encoded with multiple FPs and resistance genes, which leads to a different message depending on the growth medium employed. When ampicillin is used as the cipher, the SPAM A message correctly reads, “this is a

bioencoded message from the walt lab @ tufts university 2011”. When kanamycin is used as the cipher, the SPAM **B** message reads, “you have used the wrong cipher and the message is gibberish.” The last SPAM **C** does not produce a message because the combination of two FPs results in color emissions that do not correlate with the previously described septenary alphabet.

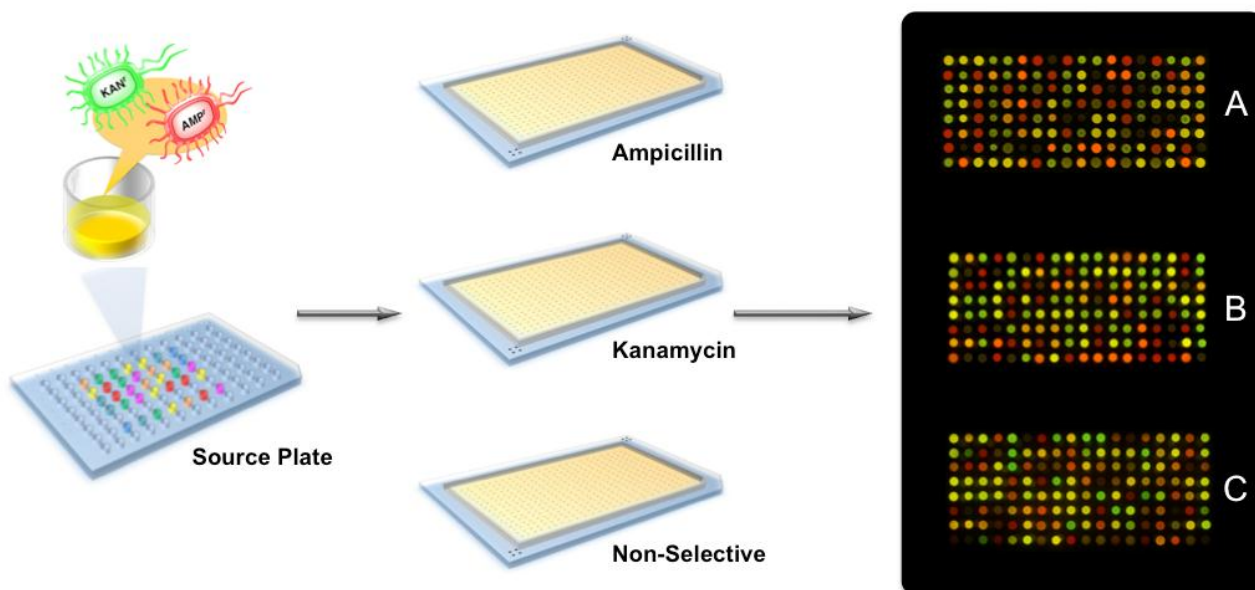


Figure 3. Scheme of SPAM messages developed from three different growth media. Selective markers are used as cipher keys with three possible outcomes. Using ampicillin as a cipher key gives SPAM **A**, which reads “this is a bioencoded message from the walt lab @ tufts university 2010”. Using kanamycin as a cipher key gives SPAM **B**, which reads “you have used the wrong cipher and the message is gibberish”. The last matrix **C** does not produce a message because the combination of two FPs results in colors that do not correlate with the septenary alphabet.

The apparent low information-density of the SPAMs is one of its major drawbacks. The most straightforward way to increase the information density would be by printing smaller features(15, 16). Furthermore, the different layers of information given by selective markers (Figure 3) can also be used to increase the information density in the array, i.e. the information density could be multiplied n -times, with n being the number of antibiotic resistant genes available. Additionally, cell lines could be designed to be resistant to a combination of antibiotics adding more dimensionality into the biological domain. Furthermore, each colony in a SPAM is a higher-order structure formed by millions of individual cells that are engaged in quorum sensing, i.e.

microbial consortium could be used to tune the expression of a fluorescent protein or possibly any other phenotype (17-19). Consequently, expanding the information density in the biological domain is limited by the number of endogenous or exogenous genes that could be engineered into an organism. In the future, another approach to increase the information density could be to encode multidimensional phenotypes, i.e. using combinations of FP chimeras. Cell lines expressing chimera FPs will generate SPAMs that can display different emission patterns that depend on the excitation wavelength used to read the message. Thus, the information density will increase in both the biological and physical domains.

This work demonstrates the use of biological systems to store and deliver information and, is the first example of using phenotypic characteristics of *living organisms* to carry and deliver an alphanumeric message. Any distinguishable phenotype could potentially be used as a signaling mechanism, as long as the expression is reliable. For this proof-of-principle, we chose to engineer laboratory strains of *E. coli*, because they are relatively straightforward and safe to handle. However, the development and viability of these microorganisms are very sensitive to environmental conditions. Future work will include extending the platform to more robust microorganisms, such as yeast (20) or endospore forming Gram-positive bacteria such as *Bacillus Subtilis* (21, 22). Using yeast will open possibilities for other types of selective markers, such as auxotrophy and/or hormonal signaling for gender selection, since yeast can reproduce asexually. Sexual reproduction could be used to add yet another level of complexity to the information system. For example, a pair of binding proteins fluorescently labeled as a FRET (Fluorescence resonance energy transfer) pair could be separately cloned into a and α strains. The mating product of these two strains will yield the FRET emission, adding a very simple optical logic gate to the system. Our labs have also begun exploring the concept of using multicellular organisms, such as plants, that could offer a longer timed-release clock and could add other useful phenotypic features as read-out signals. Finally, the large number of adjustable parameters (FPs, promoters, media, excitation wavelength, release time, etc.) makes our infobiological system a strong platform from which to explore the new field of InfoChemistry.

References

1. Glick BR, Pasternak JJ, & Patten CL (2010) *Molecular biotechnology : principles and applications of recombinant DNA* (ASM Press, Washington, DC) 4th Ed pp xvii, 1000 p.
2. Xi K & Hu J (2010) *Bio-Cryptography. Handbook of Information and Communication Security*, eds Stavroulakis P & Stamp M (Springer), pp 129-157.
3. Arita M & Ohashi Y (2004) Secret signatures inside genomic DNA. *Biotechnol Prog* 20(5):1605-1607.
4. Gibson DG, et al. (2010) Creation of a bacterial cell controlled by a chemically synthesized genome. *Science* 329(5987):52-56.
5. Bancroft C, Bowler T, Bloom B, & Clelland C (2001) Long-Term Storage of Information in DNA. *Science* 293(5536):1763-1765.
6. Clelland CT, Risca V, & Bancroft C (1999) Hiding messages in DNA microdots. *Nature* 399(6736):533.
7. Smith GC, Fiddes CC, Hawkins JP, & Cox JPL (2003) Some possible codes for encrypting data in DNA. *Biotechnol Lett* 25(14):1125-1130.
8. Yachie N, Sekiyama K, Sugahara J, Ohashi Y, & Tomita M (2007) Alignment-based approach for durable data storage into living organisms. *Biotechnol Prog* 23(2):501-505.
9. Kim C, Thomas Iii SW, & Whitesides GM (2010) Long-Duration Transmission of Information with Infofuses. *Angew. Chem. Int. Ed.* 49(27):4571-4575.
10. Hashimoto M, et al. (2009) Infochemistry: Encoding Information as Optical Pulses Using Droplets in a Microfluidic Device. *J Am Chem Soc* 131(34):12420-12429.
11. Thomas SW, et al. (2009) Infochemistry and infofuses for the chemical storage and transmission of coded information. *Proc Natl Acad Sci USA* 106(23):9147-9150.
12. Shaner NC, Steinbach PA, & Tsien RY (2005) A guide to choosing fluorescent proteins. *Nature Methods* 2(12):905-909.
13. Subach FV, et al. (2009) Monomeric fluorescent timers that change color from blue to red report on cellular trafficking. *Nat Chem Biol* 5(2):118-126.
14. Terskikh A, et al. (2000) "Fluorescent timer": protein that changes color with time. *Science* 290(5496):1585-1588.
15. Xu T, et al. (2004) Construction of high-density bacterial colony arrays and patterns by the ink-jet method. *Biotechnology and bioengineering* 85(1):29-33.

16. Merrin J, Leibler S, & Chuang JS (2007) Printing multistrain bacterial patterns with a piezoelectric inkjet printer. *PLoS ONE* 2(7):e663.
17. Brenner K, Karig DK, Weiss R, & Arnold FH (2007) Engineered bidirectional communication mediates a consensus in a microbial biofilm consortium. *Proc Natl Acad Sci USA* 104(44):17300-17304.
18. Tamsir A, Tabor JJ, & Voigt CA (2011) Robust multicellular computing using genetically encoded NOR gates and chemical. *Nature* 469(7329):212-215.
19. Regot S, et al. (2011) Distributed biological computation with multicellular engineered networks. *Nature* 469(7329):207-211.
20. Kitano H (2004) Biological robustness. *Nat Rev Genet* 5(11):826-837.
21. Romero D, Aguilar C, Losick R, & Kolter R (2010) Amyloid fibers provide structural integrity to *Bacillus subtilis* biofilms. *Proc Natl Acad Sci USA* 107(5):2230-2234.
22. Traag BA, et al. (2010) Do mycobacteria produce endospores? *Proc Natl Acad Sci USA* 107(2):878-881.